Jet-Triggered Back-Scattering Photons for Quark Gluon Plasma Tomography

Somnath De[1,2], Rainer J. Fries[1], and Dinesh K. Srivastava[2]

[1]*Cyclotron Institute and Department of Physics and Astronomy,*
Texas A&M University, College Station, TX 77845, USA and
[2]*Variable Energy Cyclotron Center, Kolkata, India*

High energy photons created from back-scattering of jets in quark gluon plasma are a valuable probe of the temperature of the plasma, and of the energy loss mechanism of quarks in the plasma. An unambiguous identification of these photons through single inclusive photon measurements and photon azimuthal anisotropies has so far been elusive. We estimate the spectra of back-scattering photons in coincidence with trigger jets for typical kinematic situations at the Large Hadron Collider and the Relativistic Heavy Ion Collider. We find that the separation of back-scattering photons from other photon sources using trigger jets depends crucially on our ability to reliably estimate the initial trigger jet energy. We estimate that jet reconstruction techniques in heavy ion experiments need to be able to get to jet $R_{AA} \gtrsim 0.7$ in central collisions for viable back-scattering signals.

I. INTRODUCTION

Electromagnetic radiation has a long history as an excellent probe in high energy nuclear collisions. The long mean free path of photons and dileptons, an order of magnitude larger than the transverse size of the colliding nuclei, allows them to carry information from the earliest stages of the collision and from deep inside the fireball to the detector systems. Over the years, several distinct sources of direct photons have been identified and calculated. They include (i) prompt photons from initial hard processes between beam partons and from jet fragmentation [1–3], (ii) pre-equilibrium photons from the secondary scatterings between partons before the system thermalizes [4], (iii) photons from jets interacting with QGP [5–7], (iv) thermal radiation from equilibrated or near-equilibrium quark gluon plasma (QGP) [8–11], (v) photons associated with the hadronization process [12], and finally (vi) thermal photons from the hot hadronic gas phase [8, 13]. These direct photons have to be experimentally separated from a large amount of background photons from hadronic decays (most notably from neutral pions).

Thermal photons, dominant at low transverse momenta p_T, are supposed to act as a thermometer of the hot nuclear matter, and there is mounting evidence that the early temperatures extracted are above the critical temperature T_c expected for the phase transition to quark gluon plasma [14, 15]. Photons from interactions of jets with QGP carry important complementary information. Hence it is critical to experimentally separate the contributions from different photon sources as much as possible so each can be analyzed appropriately. The list of photon sources in the previous paragraph follows a rough hierarchy of typical transverse momenta of the source, from high to low p_T. Jet-medium photons have been shown to make significant contributions at intermediate p_T around ~ 4 GeV/c in single inclusive photon spectra both at the Relativistic Heavy Ion Collider

(RHIC) and the Large Hadron Collider (LHC), but they compete with prompt hard photons at larger p_T and thermal and pre-equilibrium photons at smaller p_T. Hence it has been hard to confirm their existence from measurements of single inclusive photon spectra alone, much less to exploit their properties. Elliptic flow of jet-medium photons had been predicted to be negative and it was expected to serve as a telltale signature [16, 17]. However experimental studies of direct photon v_2 have not been able to bring conclusive evidence for the existence of jet-medium photons [18, 19].

In this work we propose to use the correlation of large momentum photons with jets in the opposite direction to measure the strength of a part of the jet-medium photon source, more precisely the photons from back-scattering kinematics. We will argue that this effectively rids the sample of photons from thermal and pre-equilibrium sources and vastly reduces the background from jet fragmentation photons. Furthermore, energy loss of the parent parton should shift back-scattering photons toward smaller momenta, exposing them compared to the remaining background source of prompt hard photons which are not affected by parton energy loss. On the other hand, energy loss of the trigger jet, and the experimental uncertainty measuring jet energies tend to wash out the signal from back-scattering photons. We will discuss these effects in detail below. Great opportunity awaits us if we successfully measure the strength of the back-scattering process. Besides having a complementary measure of parton energy loss independent of hadronic measurements (quarks will lose energy before converting into photons), one could measure the temperature of the medium ($T \sim 200$ MeV) independently using back-scatter photons with energies of tens of GeV.

Jet-medium photons have most notably been calculated in two limits: as electromagnetic bremsstrahlung to jet quenching [7, 11], e.g. in the Arnold-Moore and Yaffe (AMY) approach, and as an elastic back scattering process [5]. The latter is based on the fact that $2 \rightarrow 2$

Compton and annihilation scattering with a photon in the final state, $q+g \to \gamma+q$ and $q+\bar{q} \to \gamma+g$ both have a sharp peak at backward angles. In other words, when a fast quark annihilates with a slow antiquark, or Compton scatters off a slow gluon from the thermal medium, in most of the cases (Compton) or in about half the cases (annihilation) the photon created carries approximately the momentum of the fast quark. Back-scattering processes of this type are well known and are exploited in numerous ways, e.g. to create high energy photon beams. In photon beam facilities laser photons (typically ~ 1 eV) are Compton back-scattered from a high energy electron beam (in the MeV to GeV range) to create collimated beams of MeV to GeV photons [20, 21]. The QCD Compton analogue that we use here consists of a thermal gluon (~ 200 MeV) scattering off a quark (~ 20 GeV) to produce a ~ 20 GeV photon. Both bremsstrahlung and back-scattering calculations are often carried out in a leading parton approximation to jets in a medium [5] however more general calculations using the parton dynamics inside a jet shower in a medium have recently become available [22].

II. CALCULATING PHOTON SOURCES

In Ref. [5] the rate of Compton and annihilation processes between one parton from a set of fast quarks subject to energy loss, and another from a fireball with a temperature profile $T(x) = T(\tau, \eta, \mathbf{x}_\perp)$ was calculated in the backward peak approximation ($\mathbf{p}_\gamma \approx \mathbf{p}_{\text{fast } q}$) to be

$$E_\gamma \frac{dN}{d^4x d^3p_\gamma} = \frac{\alpha\alpha_s}{4\pi^2} \sum_{q=1}^{N_f} \left(\frac{e_q}{e}\right)^2 T^2(x)$$
$$\times \left[f_q(\mathbf{p}_\gamma, x) + f_{\bar{q}}(\mathbf{p}_\gamma, x)\right] \left[\ln \frac{3E_\gamma}{\alpha_s \pi T(x)} + C\right], \quad (1)$$

where $C = -1.916$. Here α and α_s are the electromagnetic and strong coupling constant respectively. f_q is the phase space distribution of fast quarks interacting with the medium and e_q is the electric charge of a quark with the index q running over all active quark flavors. This formula is easily generalized to the rate of photons associated with a trigger jet whose energy, pseudorapidity and relative azimuthal angle, E_T, y_j, ϕ_j, fall within a trigger window $\mathcal{T}_j$ in E_T-y_j-ϕ_j space. For the latter we replace the single inclusive parton distribution $f_q(\mathbf{p}_\gamma, x)$ by the parton-jet pair distribution integrated over $\mathcal{T}_j$,

$$f_q^{\mathcal{T}_j}(\mathbf{p}_q, x) = \frac{(2\pi)^3}{g_q \tau p_T} \delta(y - \eta)\rho(\tau, \mathbf{x}_\perp^0)$$
$$\times \int_{\mathcal{T}_j} dE_T dy_j d\phi_j E_q \frac{dN}{d^3p_q dE_T dy_j d\phi_j}\bigg|_{\substack{\mathbf{p}_q^0 = \mathbf{p}_q + \Delta\mathbf{p}_q \\ E_T^0 = E_T + \Delta E_T}}.$$
$$(2)$$

Here $x = (\tau, \eta, \mathbf{x}_\perp)$ and $\mathbf{p}_q$ are the position and momentum of the quark at the time of the back scatter-

ing and $x^0 = (\tau_0, \eta, \mathbf{x}_\perp^0)$ and $\mathbf{p}_q^0$ are the original position and momentum when the quark was created in a hard process. Propagation is assumed to be along straight lines in the direction of $\mathbf{p}_q$ with the speed of light, i.e. $\mathbf{x}_\perp = \mathbf{x}_\perp^0 + (\tau - \tau_0)\hat{\mathbf{p}}_q^0$. $\Delta\mathbf{p}_q = \mathbf{p}_q^0 - \mathbf{p}_q$ is the energy lost between $\mathbf{x}_\perp^0$ and $\mathbf{x}_\perp$. Straight line propagation implies that $\Delta\mathbf{p}_q$ is collinear with the original momentum of the quark. Similarly ΔE_T is the energy lost by the trigger jet in the medium. ΔE_T will strongly depend on the cone size chosen in the experimental reconstruction of the jet. $g_q = 6$ is the spin and color degeneracy factor of quarks and ρ is the density of nucleon-nucleon collisions in the transverse plane.

We have to consider the background from prompt hard photons and fragmentation photons with an awayside jet in the same trigger window $\mathcal{T}_j$. We will not consider trigger windows with jet E_T smaller than 20 GeV. The pre-equilibrium and thermal photons do not possess back-to back correlation with an away-side jet, hence can be eliminated from the background. We can thus compute the nuclear modification factor R_{AA} of photons with an awayside high energy trigger jet as:

$$R_{AA} = \frac{(\text{backscat.} + \text{prompt hard} + \text{fragment.})_{A+A}}{N_{\text{coll}} \times (\text{prompt hard} + \text{fragment.})_{p+p}}$$
$$(3)$$

where N_{coll} as usual is the total number of binary nucleon-nucleon collisions.

Our calculation comprises two stages. At the first stage we calculate the background (prompt hard and fragmentation) photon and parton (prior to back-scattering) cross sections at leading order (LO) or next-to-leading order (NLO) in α_s in the code JETPHOX (version 1.2.2) [2, 3]. The default will be LO cross sections unless explicitly stated otherwise. We use CTEQ6M [23] parton distributions for protons and EPS09 modifications for nuclei [24] in JETPHOX.

For the second stage we use the code package PPM [25, 26] to calculate (i) the energy loss of partons, (ii) the energy loss of jets, and (iii) the back-scattering photon rate according to Eq. (1). PPM propagates partons and jets (represented by their leading parton) through a fireball model. Here this is done pairwise, i.e. photon-jet pairs and quark-jet pairs propagate from their point of creation though a hard parton-parton scattering. The spatial distribution ρ of hard processes is given by the nucleon-nucleon collision density from a Glauber calculation. For photon-jet pairs the energy loss of the jet due to its path through the medium is calculated, and all photon-jet pairs with a final jet energy within $\mathcal{T}_j$ are counted as part of the background. We do not take into account energy loss of partons before fragmentation into photons which will lead to a lower bound for the signal to background ratio. If energy loss of partons for photon fragmentation were taken into account in addition, it would help to suppress the fragmentation background at high photon-z where z is the momentum fraction of

the parent parton carried by the photon. For quark-jet pairs the energy loss of the jet and of the parton are computed while the back-scattering probability of the parton is also computed along the way. All final photons from this source which lie in $\mathcal{T}_j$ are counted as part of the photon signal.

Our fireball model describes a longitudinally expanding, boost-invariant QGP phase. The transverse profile of the entropy density is fixed by the participant density of nucleons from a Glauber calculation. We do not expect our main conclusions to change much if transverse expansion or fluctuations in the fireball are taken into account. The normalization of the entropy density is fixed by data from RHIC [27] and scaled up to describe multiplicity data in Pb+Pb collisions at the LHC. We use a relativistic ideal gas equation of state for 3 light quark flavors to calculate the temperature needed in the photon conversion formula. This procedure will slightly underestimates the real temperature and thus the photon production rate at a given value of the entropy density s, in particular close to the pseudo-critical temperature T_c.

The energy loss of quarks and gluons is calculated from a simple LPM-inspired approximation (called sLPM in Ref. [25]) which uses $dp_T/d\tau = -\hat{q}(\tau - \tau_0)$ where the value of $\hat{q}$ is proportional to the local entropy density s of the fireball at that space-time point. The proportionality constant is fitted to simultaneously describe RHIC and LHC data on single inclusive hadron suppression. Despite its simplicity, this model describes basic features of high momentum hadron production at RHIC reasonably well [25]. The resulting initial value of $\hat{q} \approx 1.2$ GeV^2/fm in the center of Au+Au collisions at RHIC energy is consistent with recent findings of the JET collaboration [28].

Jet energy loss is much less under theoretical control. A consistent calculation can only be done with a full jet shower simulation in the medium, e.g. [22]. Here we choose a simple model of the path length and energy dependence to reproduce gross features of jet energy loss. We parameterize that the energy loss (i.e. the amount of energy outside of a given jet cone) is proportional to path length, and we add a small energy dependence, $dE_T/d\tau = -\hat{r}\ln(E_T/\Lambda)$ where $\Lambda = 0.2$ GeV. $\hat{r}$ is proportional to the local entropy density s as in the case of leading parton energy loss. The linear path length dependence appears more appropriate both for the stochastic process of stripping partons off the jet cone as the jet goes through the medium, and for the large angle radiation with short formation times that plays a role as well. The normalization of $\hat{r}$ is varied to obtain different inclusive jet R_{AA}.

III. RESULTS

In order to calibrate jet energy loss we calculate the nuclear modification factor R_{AA} of single inclusive jets for both central Au+Au collisions at RHIC energy and central Pb+Pb collisions at LHC energy in our jet energy
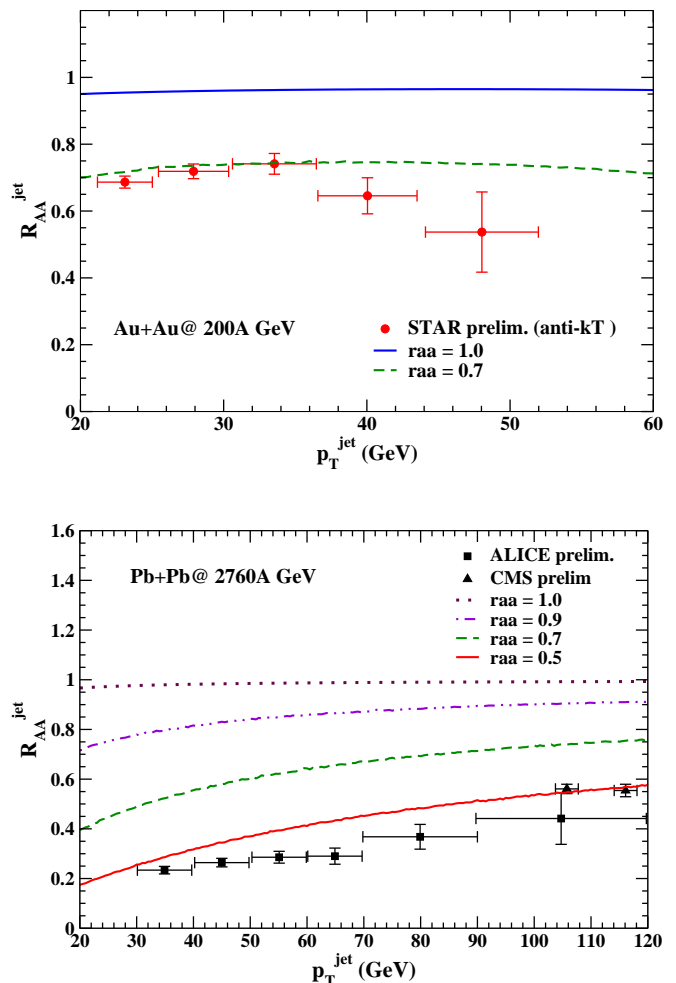

FIG. 1: (Color online) Upper Panel: R_{AA} of single inclusive jets as a function of jet p_T in central Au+Au collisions at RHIC for two values of $\hat{r}$ corresponding to "raa" values of roughly 1.0 ($\hat{r} = 0$) and 0.7 at 30 GeV respectively. Lower Panel: The same for central collisions of lead nuclei at LHC energy, for four values of $\hat{r}$, corresponding to raa values of roughly 1.0, 0.9, 0.7 and 0.5 at 100 GeV respectively. Data from the STAR [29], ALICE [30] and CMS [31] collaborations for jet cone radii of 0.4, 0.2 and 0.4 respectively, are also shown for comparison.

loss model. This allows us to scale the normalization of the parameter $\hat{r}$ to reproduce a certain inclusive jet R_{AA}. We will refer to different values of jet energy loss by quoting the approximate value of R_{AA} at $E_T = 30$ GeV for RHIC and $E_T = 100$ GeV at LHC, respectively. We will quote this number in plots as "raa". Fig. 1 shows the single inclusive R_{AA} for jets corresponding to values of raa of roughly 1, 0.9, 0.7 and 0.5 for central Pb+Pb collisions at LHC and 1.0 and 0.7 for central Au+Au collisions at RHIC, respectively. We also show the data from STAR, ALICE and CMS that use rather small jet cone radii of 0.4, 0.2 and 0.4, respectively. Without a full jet shower simulation we can not make a rigorous connec-

tion between jet cone radius, jet quenching, and jet R_{AA}. Rather we will present our results using a set of different values of "raa" (and thus $\hat{r}$). As can be seen from the figure the lowest values of raa for both RHIC (0.7) and LHC (0.5) roughly correspond to the suppression seen in current data with small cone radii. With improving jet reconstruction techniques and larger jet cone radii larger values of "raa" might become feasible. Small jet cones in heavy ion experiments are mostly dictated by the relatively large background that needs to be subtracted. The value of $\hat{r}$ needed to reproduce raa of 0.7 at RHIC is about 0.24 GeV/fm initially in the center of head-on Au+Au collisions which corresponds to an initial energy loss of ~ 1.2 GeV/fm for 30 GeV jets.

We can now proceed to calculate photon spectra opposite of trigger jets in several scenarios. For this preliminary study we choose the trigger window $\mathcal{T}_j$ for the jet to be defined as $-1 < y_j < 1$ and 30–35 GeV in E_T for RHIC, and $-2 < y_j < 2$ and 60–65 GeV in E_T for LHC. We define the away-side as an angle between 165 and 195 degrees in relative azimuthal angle. Let us briefly discuss the choice of trigger window. The yield of single-inclusive back-scattering photons falls faster with p_T than prompt hard photons (similar to a higher twist contribution in perturbative QCD), thus the signal will become stronger with smaller p_T. However, experiments need to be able to reconstruct jets in a reliable manner. This puts a lower bound on the trigger window E_T. Our choice is an attempt to maximize the back-scattering yield while keeping jet reconstruction feasible. We would also like to make our back-scattering signals as sharply defined as possible, which is ideally achieved with very narrow trigger windows. However, uncertainties in the jet energy reconstruction put constraints on the energy resolution achieved in experiments. We have chosen a trigger window width of 5 GeV for this study.

Fig. 2 shows our results for jet-triggered photon spectra in central Au+Au collisions at RHIC for scenarios with jet raa 1.0 and 0.7 at leading-order (LO) accuracy. At LO and without trigger energy loss (raa 1.0) the prompt hard photon kinematics is completely determined by the trigger jet energy and leads to a well-defined band of photons between 30 and 35 GeV in transverse momentum. Fragmentation photons generally provide a low-level background just below the trigger window (they correspond to very high-z photons). We use BFG-II fragmentation function for photons [32]. The kinematic range of back-scattering photons (the signal) calculated under the same assumptions (LO, raa 1.0) and without energy loss of partons, coincide with those of prompt hard photons, as expected, although their strength is lower by about an order of magnitude. If parton energy loss is switched on with parameters determined from single hadron suppression, the back-scattering signal develops a shoulder of about 4 GeV width, indicating that quarks have lost up to 4 GeV of energy before conversion to photons. This pushes some back-scattering photon strength into the region of fragmentation photons which makes for a much better
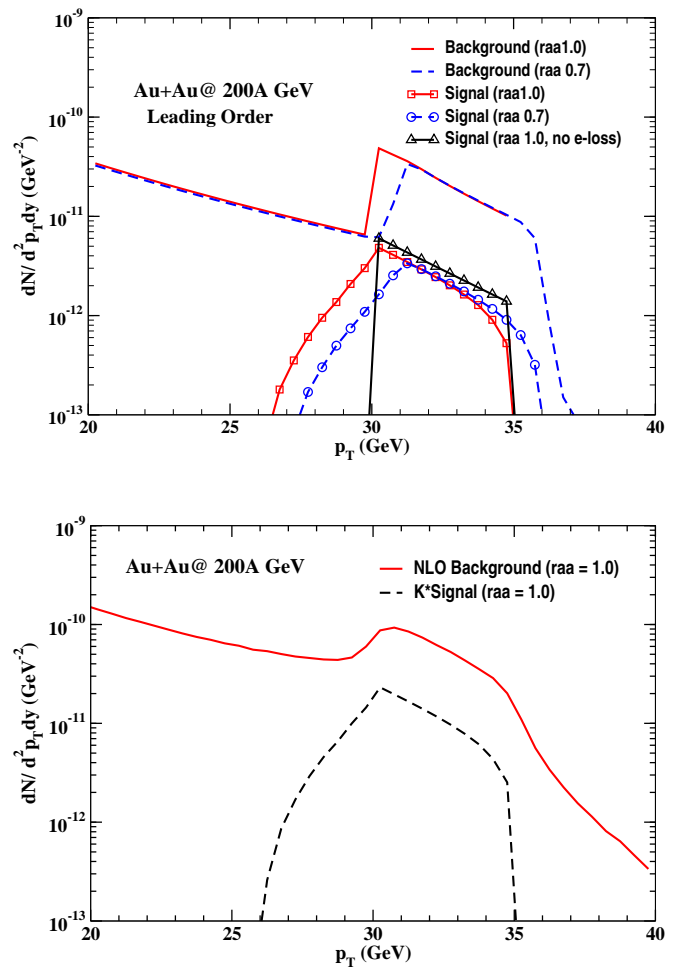

FIG. 2: (Color online) Upper Panel: Yield dN/d^2p_Tdy of photons opposite of a jet with energy between 30 and 35 GeV in central Au+Au collisions at $\sqrt{s_{NN}} = 200$ GeV. We show the sum of prompt hard photons and fragmentation photons (solid and dashed line) and back-scattering photons (solid lines with marks) at LO accuracy for the hard process for different parton and trigger energy loss scenarios. Triangles: signal for no parton energy loss and no trigger jet energy loss (raa 1.0). Squares: parton energy loss on, no trigger jet energy loss (raa 1.0). Circles: both parton energy loss and trigger jet energy loss at realistic strength (raa 0.7). Lower Panel: The same as upper panel, however background (prompt hard + fragmentation) calculated at NLO accuracy for the case raa 1.0 (solid line). Back-scattering photons for raa 1.0 (dashed line) at LO accuracy multiplied by a K-factor.

signal/background ratio just below the trigger window.

If jet energy loss is taken into account in addition, with cone radii currently available (raa 0.7), both the hard prompt photon background and the back-scattering photon spectra become slightly more diffuse and tend to be shifted to higher p_T since a trigger jet measured between 30-35 GeV might have originated as a jet with larger energy. The jet triggered photon spectra thus carry fairly obvious information about the energy loss of partons and
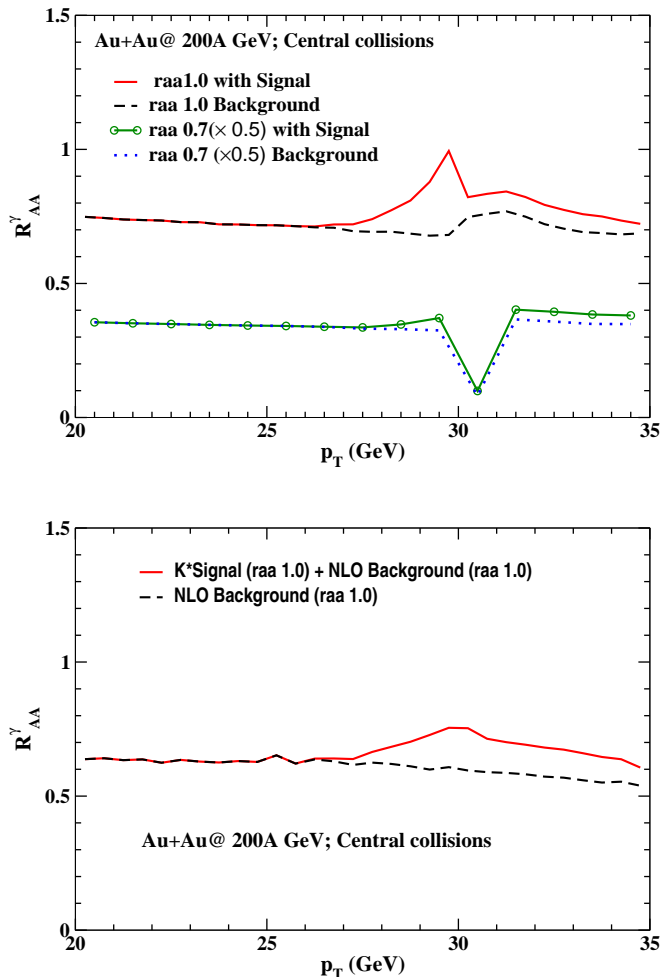
FIG. 3: (Color online) Upper Panel: Nuclear modification factor R_{AA} calculated from the results in Fig. 2 for background and signal at LO accuracy for (i) jet raa 1.0 and (ii) jet raa 0.7 (scaled by 0.5 for better visibility). In both cases (signal+background)/background and the reference background/background are shown. Lower Panel: The same as the upper panel but for raa 1.0 at NLO accuracy.

trigger jets in their broadening around the trigger window.

These strong kinematic correlations are washed out by NLO corrections to the hard process in which another hard parton can be emitted in the final state. The effect is estimated in the lower panel of Fig. 2 where the background is now calculated at NLO accuracy and raa 1.0. We also show the back-scattering photons at LO accuracy but with a K factor. Our calculation of back-scattering photons in its current form is not suitable to deal with radiative corrections as it is not clear how to treat medium induced radiation of a collinear pair of quarks that would end up in the same jet cone. However our results seem to indicate that the decorrelation of the signal with the trigger window that comes from radiative corrections to the hard process is generally weaker than the decorrela-

tion that is induced by parton and trigger jet energy loss. This is even more the case at LHC energies where energy loss is large. Here the K factor is determined from the ratio (background at NLO)/(background at LO) in the fragmentation dominated region of the background. We chose to determine K at 20 GeV for RHIC and 40 GeV for LHC.

We proceed to show the results for the nuclear modification factor R_{AA}. Experimentally, R_{AA} can be determined with smaller systematic uncertainties compared to spectra, and might thus be a more promising observable. Fig. 3 shows R_{AA} as defined in Eq. (3) for central Au+Au collisions at RHIC for (i) raa 1.0 and (ii) raa 0.7 (scaled by 0.5). For comparison we also show the result one would obtain if back-scattering photons were absent (i.e. the ratio of fragmentation and prompt hard photons for Au+Au and $p + p$). The difference between the R_{AA} with and without inclusion of signal, is the signature for jet-triggered back-scattering photons.

Let us understand the key features of R_{AA}. First, we note that the nuclear modification factor of background photons (i.e. background photons in A+A vs background photons in $p + p$) is not around 1. This is because background photons at RHIC probe hard processes with quarks in the initial wave function. In A+A those processes are suppressed due to the larger fraction of d valence quarks compared to u valence quarks in nuclei and their smaller electric charge. We notice that trigger jet energy loss can lead to suppression of R_{AA} in the trigger window due to the shift of strength of background photons to larger energies. In fact the width of such a dip is related to the size of the typical jet energy loss. The signal of back-scattering photons on the other hand creates an enhancement in R_{AA} which is peaked just below the trigger window. Both the dips in the background and the enhancement due to the signal are typical effects that will also appear at LHC. In contrast, radiative effects on the distribution of background photons in the NLO calculation generally tends to smear out an enhancement due to the signal.

Fig. 4 shows the jet-triggered photon spectrum for central Pb+Pb collisions at LHC for the 60–65 GeV trigger window discussed above. We show both signal and background for the four jet energy loss scenarios (raa 1.0, 0.9, 0.7 and 0.5) at LO kinematics with parton energy loss included. All the features discussed for the RHIC case are qualitatively present at LHC as well. However, the diffusion of signal strength both due to parton energy loss and jet energy loss is much larger than at RHIC for the raa 0.7 and 0.5 scenarios, creating shoulders up to 15–20 GeV wide on both sides of the trigger window.

Fig. 5 shows R_{AA} for trigger energy loss scenarios raa 1.0, raa 0.7, and raa 0.5. The baseline suppression due to d valence quarks is not present at LHC where hard processes are dominated by gluon fusion. We again find dips in the background R_{AA} in the trigger window due to trigger energy loss, and enhancement in R_{AA}, peaked below the trigger window, from back-scattering photons.
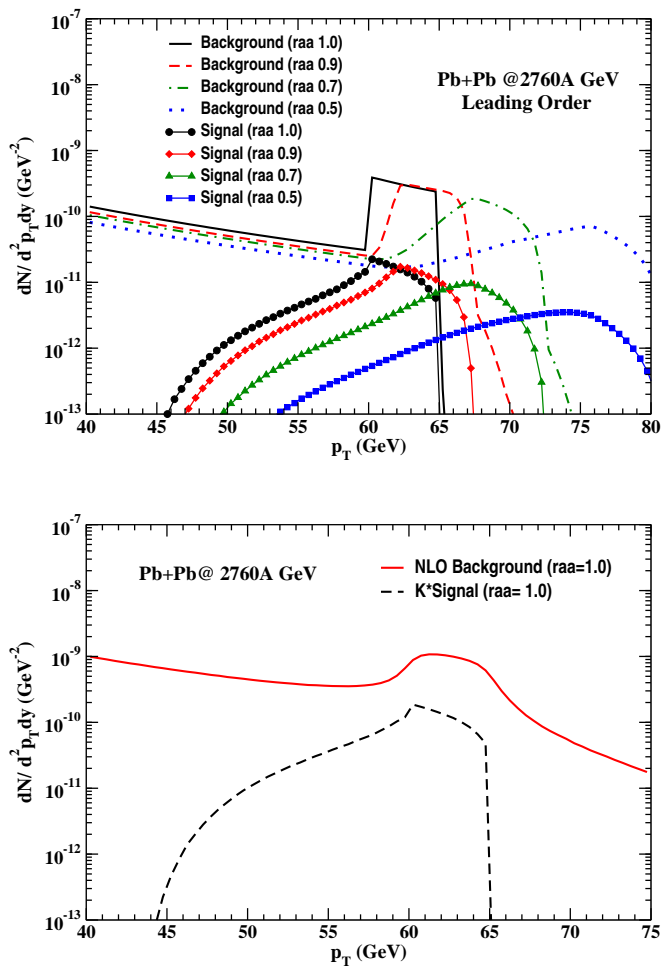
FIG. 4: (Color online) Upper panel: The same as Fig. 2 for trigger jets between 60 and 65 GeV energy in central Pb+Pb collisions at $\sqrt{s_{NN}} = 2760$ GeV for four different trigger jet energy loss scenarios: raa 1.0 (solid line, circles), raa 0.9 (dashed line, diamonds), raa 0.7 (dash-dotted line, triangles), 0.5 (dotted line, squares). Both background and back-scattering signal are calculated at LO accuracy for the hard process. All scenarios have parton energy loss taken into account. Lower panel: Background (prompt hard + fragmentation) is calculated at NLO accuracy for the case raa 1.0 (solid line) while back-scattering photons are estimated at LO accuracy for raa 1.0 (dashed line), multiplied by a K-factor.

While raa 1.0 shows a rather promising signature peak the signal for the more realistic raa 0.5 and raa 0.7 jet energy loss scenarios are small.

IV.   SUMMARY AND DISCUSSION

We have, for the first time, calculated the correlation of medium-induced photon radiation from jets with trigger jets. We have focused on back-scattering photons from the Compton process. Our numerical studies indicate that there is a potential signal from back-scattering
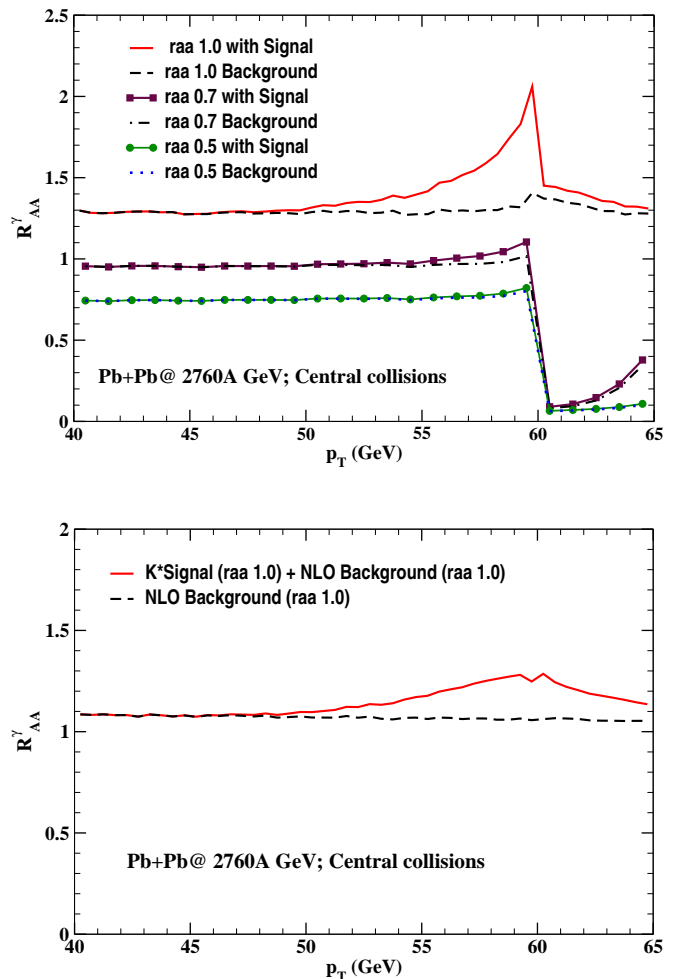
FIG. 5: (Color online) Upper panel: Nuclear modification factor R_{AA} for central collisions of lead nuclei at LHC at LO accuracy for raa 1.0, raa 0.7 and raa 0.5. We again show R_{AA} with and without the inclusion of back-scattering photons. Lower panel: The same calculated for raa 1.0 at NLO accuracy.

photons in the R_{AA} of photons opposite of trigger jets in high energy nuclear collisions. The signal is mostly due to a downward shift of back-scattering photons in momentum due to parton energy loss before the back-scattering occurs. This reduces the background from prompt hard photons significantly. However, trigger jet energy loss and radiative corrections to the underlying hard processes tend to wash out the correlation. The decorrelation of signal and trigger due to jet energy loss dominates over those due to NLO corrections at LHC energies. With the currently used small jet cone radii and the typical trigger jet R_{AA} measured at RHIC and LHC the signal is visible in our calculation, but it would be too small to be seen experimentally.

We should emphasize here that many features of our calculation are designed to establish a *lower* bound on the signal strength and a more detailed follow-up calcu-

lation could lead to a more promising result. Here are the main points that establish a lower bound: (i) The simple equation of state underestimates the temperature and thus the back-scattering rate. (ii) We omitted induced photon bremsstrahlung, which will generally increase the signal photon rate below the trigger window. Obviously back-scattering photons have the advantage of a rather sharp feature in R_{AA}, while additional yield which simply scales up R_{AA} in a p_T-independent way will be harder to find experimentally. (iii) Photon fragmentation might happen partially or fully outside of the medium. In that case fragmentation photons are subject to energy loss which is neglected here. This effect will shift the background from fragmentation towards smaller p_T, effectively decreasing the background. We have also not systematically explored different kinematic cuts on the trigger jet or the photon that could possibly improve the signal over background ratio. Nevertheless we conclude that single inclusive jet R_{AA} of 0.7 or larger in central collisions will likely be necessary to carry out this measurement.

Going beyond the back-scattering peak approximation in Eq. (1) leads to decorrelation of the trigger and back-scattering photon, however, it will also tend to push some of the signal strength to lower p_T, away from the prompt hard photon background. The net effect might thus not be simply a loss of signal due to decorrelation. In principle our proof-of-principle calculation could be improved in several ways. A full jet shower Monte-Carlo would remove the need for a leading parton approximation. It could also mimic NLO kinematics which we have only employed when final state effects leading to energy loss is absent since no consistent theory is available in that case.

One could consider the use of high-p_T trigger hadrons instead of trigger jets. They will be subject to the parton energy loss and jet energy loss which leads to smearing of the back-to-back energy correlation as discussed in the jet-photon case. In addition, there is smearing due to the fragmentation of the hadron which by itself already almost completely destroys the correlation in energy with the photon on the other side, see e.g. [33]. Therefore hadron triggered photons have not been considered here.

[1] J. F. Owens, Rev. Mod. Phys. **59**, 465 (1987).
[2] S. Catani, M. Fontannaz, J. P. Guillet and E. Pilon, JHEP **0205**, 028 (2002).
[3] P. Aurenche, M. Fontannaz, J. -P. Guillet, E. Pilon and M. Werlen, Phys. Rev. D **73**, 094007 (2006).
[4] S. A. Bass, B. Muller and D. K. Srivastava, Phys. Rev. Lett. **90**, 082301 (2003).
[5] R. J. Fries, B. Muller and D. K. Srivastava, Phys. Rev. Lett. **90**, 132301 (2003).
[6] R. J. Fries, B. Muller and D. K. Srivastava, Phys. Rev. C **72**, 041902 (2005).
[7] B. G. Zakharov, JETP Lett. **80**, 1 (2004) [Pisma Zh. Eksp. Teor. Fiz. **80**, 3 (2004)].
[8] J. I. Kapusta, P. Lichard and D. Seibert, Phys. Rev. D **44**, 2774 (1991) [Erratum-ibid. D **47**, 4171 (1993)].
[9] R. Baier, H. Nakkagawa, A. Niegawa and K. Redlich, Z. Phys. C **53**, 433 (1992).
[10] P. Aurenche, F. Gelis, R. Kobes and H. Zaraket, Phys. Rev. D **58**, 085003 (1998).
[11] P. B. Arnold, G. D. Moore and L. G. Yaffe, JHEP **0112**, 009 (2001).
[12] G. Chen, R. J. Fries, *in preparation*.
[13] S. Turbide, R. Rapp and C. Gale, Phys. Rev. C **69**, 014903 (2004).
[14] A. Adare *et al.* [PHENIX Collaboration], Phys. Rev. Lett. **104**, 132301 (2010).
[15] M. Wilde [ALICE Collaboration], Nucl. Phys. A904-905 **2013**, 573c (2013).
[16] S. Turbide, C. Gale and R. J. Fries, Phys. Rev. Lett. **96**, 032303 (2006).
[17] S. Turbide, C. Gale, E. Frodermann and U. Heinz, Phys. Rev. C **77**, 024909 (2008).
[18] A. Adare *et al.* [PHENIX Collaboration], Phys. Rev. Lett. **109**, 122302 (2012).
[19] D. Lohner [ALICE Collaboration], J. Phys. Conf. Ser. **446**, 012028 (2013).
[20] R. H. Milburn, Phys. Rev. Lett. **10**, 75 (1963).
[21] F. R. Arutyunian and V. A. Tumanian, Phys. Lett. **4**, 176 (1963).
[22] T. Renk, Phys. Rev. C **88**, 034902 (2013).
[23] J. Pumplin *et al.* JHEP **0207**, 012 (2002).
[24] K. J. Eskola, H. Paukkunen and C. A. Salgado, JHEP **0904**, 065 (2009).
[25] R. Rodriguez, R. J. Fries and E. Ramirez, Phys. Lett. B **693**, 108 (2010).
[26] R. J. Fries and R. Rodriguez, Nucl. Phys. A **855**, 424 (2011).
[27] S. Pal and S. Pratt, Phys. Lett. B **578**, 310 (2004).
[28] K. M. Burke *et al.*, Phys. Rev. C **90** 014909 (2014).
[29] M. Ploskon [STAR Collaboration], Nucl. Phys. A **830**, 255C (2009).
[30] R. Reed [ALICE Collaboration], J. Phys. Conf. Ser. **446**, 012006 (2013).
[31] M. Belt Tonjes [CMS Collaboration], Nucl. Phys. A **904-905**, 713c (2013).
[32] L. Bourhis, M. Fontannaz and J. P. Guillet, Eur. Phys. J. C **2**, 529 (1998).
[33] G. Y. Qin, J. Ruppert, C. Gale, S. Jeon and G. D. Moore, Eur. Phys. J. C **61**, 819 (2009).